


Ultra low-field-emission stretchable electroluminescent devices enabled by a transparent and high- κ dielectric gel

Received: 8 May 2025

Zupeng Liu^{1,3}, Zhao Liu^{2,3}, Xia Lei¹, Yujue Yang¹✉ & Titao Jing¹✉

Accepted: 3 November 2025

Published online: 17 December 2025

 Check for updates

Stretchable displays are the key components for next-generation flexible electronics, playing a critical role in interactive human–machine interfaces. Stretchable alternating current electroluminescent devices, one of the most promising methods for achieving stretchable displays, face challenges such as high driving alternating voltages and frequencies. Herein, we employ a high- k dielectric gel as the emitting matrix, enabling a stretchable electroluminescent device with a turn-on voltage of 13 V ($0.19 \text{ V } \mu\text{m}^{-1}$) at 50 Hz and a maximum luminance of 1944.7 cd m^{-2} at $2.5 \text{ V } \mu\text{m}^{-1}$ with 1 kHz. Moreover, the gel-based devices exhibit a high elongation up to 600%. We further employ fluorescent electrodes to achieve multi-color display of Yellow, Green, and Red without complicated structures. We also assemble a colorful display capable of dynamically exhibiting real-time information. These features highlight the material's considerable performance and demonstrate its transformative potential for wearable electronics and next-generation flexible displays.

The swiftly evolved flexible electronics have demonstrated great potential in remolding the lifestyle of human beings^{1–4}. As a crucial component of electronics, optical displays have spurred numerous applications in stretchable devices, such as visual read-out, optical communication and neurostimulation, and soft robotics^{5–10}. To date, several mechanisms, including light-emitting diodes (LEDs) and alternating-current electroluminescent (ACEL) devices, have been proposed to achieve stretchable optical displays^{4,11–13}. The LEDs, including organic light-emitting diodes (OLEDs), quantum dot light-emitting diodes (QLEDs), feature high luminance^{5,14,15}. Unfortunately, their stretchability is still a great challenge even though remarkable progress has been made in recent years^{7,15,16}. In addition, the LEDs require a balanced charge injection for emission, which imposes strict requirements on materials and assembly process^{1,5}. In contrast, the ACEL devices can easily achieve excellent and intrinsic stretchability by using a light-emitting layer of ZnS phosphors embedded in elastomer^{17–19}. The typical structure of ACEL devices consists of two stretchable electrodes sandwiching a light-emitting layer with a low interface requirement^{13,20}. The structure is very simple as compared with that of the LEDs, enabling

ACEL devices suitable for versatile stretchable optoelectronics, from films to textiles, for various scenarios^{20–24}.

Despite numerous merits, the driving of ACEL devices usually requires high alternating electric fields (E) at high frequency to excite the ZnS phosphors, because of the low dielectric constant (k) of the elastomer^{11,17,25}. Such driving requirements pose significant challenges to portable devices and raise safety concerns when the ACEL devices are applied for human–machine interactions¹¹. A fundamental principle of employing high- k substrates to enhance luminance has been well-established in the industry for ACEL devices. However, the transition to stretchable electronics has revealed an unexpected issue: while the principle remains valid, its implementation becomes profoundly challenging. To achieve stretchability, researchers must employ elastomeric matrices, which typically exhibit dielectric constants below $10^{26,27}$. Hence, researchers have put great effort to explore transparent and high- k elastomer, aiming at reducing the operating requirements of the stretchable ACEL devices^{11,25,28–30}. One breakthrough occurred in 2019, Tan et al. prepared a plasticized fluoroelastomer and demonstrated the record-low turn-on electric field of $0.34 \text{ V } \mu\text{m}^{-1}$ with 50 Hz¹¹. The total

¹School of Chemical Engineering and Technology, Sun Yat-sen University, Zhuhai, China. ²Department of Materials Science and Engineering, Monash University, Victoria, Australia. ³These authors contributed equally: Zupeng Liu, Zhao Liu. ✉ e-mail: yujue1031.yang@connect.polyu.hk; jingtt@mail.sysu.edu.cn

elongation of the ACEL device achieves up to 800%. Nevertheless, the recoverable elongation of the plasticized fluoroelastomer is only 50%. The ACEL devices are hard to recover after a large elongation. Besides, the color capability is also a major obstacle for the stretchable ACEL devices because of the limitation of phosphors^{5,31}.

Herein, we present a stretchable ACEL device based on a high- k and stretchable gel dielectric, as shown in Fig. 1a. The devices exhibit a turn-on electric field as low as $0.19 \text{ V } \mu\text{m}^{-1}$ at 50 Hz. Moreover, the stretchability of the light-emitting layer is inherited from an intrinsically stretchable gel rather than plasticized polymers, enabling the devices with an elongation up to 600%. We also employ fluorescent electrodes for multi-color displays without additional or complicated structure designs. Through the light conversion of the photoluminescence, the

initial Blue color is extended to Yellow, Green, and Red colors with high luminance. The stretchable ACEL devices possess a brightness up to $1944.7 \pm 99.4 \text{ cd m}^{-2}$ at $2.5 \text{ V } \mu\text{m}^{-1}$ of 1 kHz, indicating a considerable achievement in stretchable display. Subsequently, we assemble a wearable display device of 128 pixels powered by a battery. The wearable display can dynamically display information through wireless communication in real time, illustrating the promising potential for human-machine interaction as a wearable display device.

Results and discussion

Transparent and high- κ gel enables bright ACEL devices

The dielectric constant, transparency, elastic stretchability, and space for ZnS loading are the four key characteristics for the

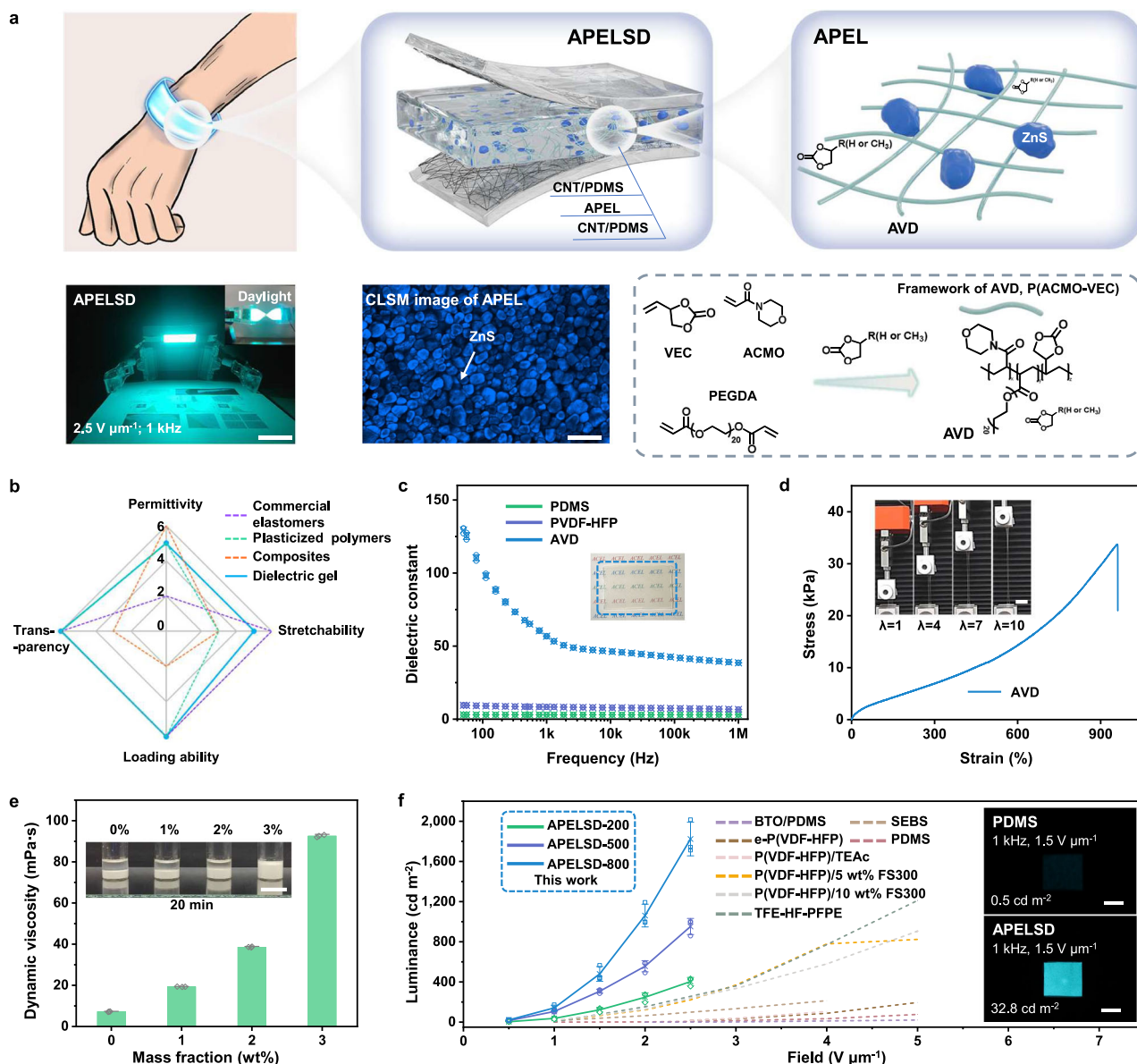


Fig. 1 | High- k and stretchable dielectric gel as the emitting layer matrix for bright ACEL devices. **a** Structure of stretchable APELSD. The digital photos are obtained by an APELSD excited at $2.5 \text{ V } \mu\text{m}^{-1}$ with 1 kHz (scale bar, 5 cm). The CLSM image of the emitting layer, APEL, is also presented (scale bar, $60 \mu\text{m}$). **b** The comparison of the different dielectrics in four dimensions for stretchable ACEL devices. **c** The dielectric constants of AVD compared to those of other stretchable materials. Data points represent mean \pm SD ($n = 3$). An image of transparent AVD is also inserted. **d** The stress-strain curve of the dielectric gel. Scale bar, 2 cm.

e Dynamic viscosity of precursor liquid containing different contents of PVP. Data points represent mean \pm SD ($n = 3$). The inserted figure is the ZnS mixed precursor liquid after 20 min placement. Scale bar, 1 cm. **f** A comparison of the APELSD in this work with previously reported stretchable ACEL devices in terms of the operated electric fields and their corresponding luminance. The inserted digital photos are the APELSD and silicone-based device with $70 \mu\text{m}$ emitting layer in dark. Scale bar, 1 cm. The data points of this work represent mean \pm SD ($n = 3$).

dielectric to realize the ACEL devices with high luminance at low applied electric field. Previous studies have reported numerous dielectrics, including doped elastomer and plasticized polymers^{11,26,32,33}. But these dielectrics are hard to achieve excellent performance in all four dimensions, as shown in Fig. 1b. Commercial elastomers have good stretchability and transparency, but their dielectric constants are usually inadequate, ranging from $3 - 10^{27}$. The doped elastomers could achieve a high dielectric constant, but the limited space for ZnS particles, low transparency and stretchability impede the performance of ACEL devices^{28,29,34}. The plasticized polymers could achieve a high dielectric constant, transparency and a large space for ZnS loading. Unfortunately, the stretchability of plasticized polymers presents a challenge of very small elastic deformation, which makes it hard to recover to their initial states¹¹. Gels are well known for their intrinsic stretchability and transparency³⁵. To date, they have been widely applied as stretchable electrodes for ACEL by using ionic solutions^{36,37}. Nonetheless, the solvent for ionic solutions is usually a polar liquid with a high dielectric constant. In this regard, the gels could also be employed as a high- k dielectric if the liquid is non-ionic³⁸.

We prepared a dielectric gel (called AVD) to achieve the four key characteristics for highly stretchable and bright ACEL devices, as described in Fig. 1a and Supplementary Fig. 1a. We chose propylene carbonate (PC) and ethylene carbonate (EC) as the swelling liquid because of the high dielectric constant and high boiling point (over 240 °C)^{39,40}. The framework of the gel is the copolymer of 4-acryloylmorpholine (ACMO) and 4-vinyl-1,3-dioxolan-2-one (VEC). The ACMO provides the stretchability, and the high polar VEC enhances the dielectric constant of the framework, as shown in Supplementary Fig. 1b–d. Using density functional theory (DFT), the dipole moments of the monomer ACMO and VEC are calculated to be 2.91 and 5.58 D, respectively. The introduction of highly polar VEC into ACMO thus enhances the polarization of the framework of the gel. Besides, the dielectric gel is free of other doped particles, enabling high-content ZnS loading similar to commercial elastomers (70 wt%, elevated ZnS contents can degrade luminance due to self-blocking effects). In general, the transparent (93%@550 nm) dielectric gel with 40% liquid content achieves a very high dielectric constant of 56.8@1 kHz, and a stretchability of over 960%, demonstrating excellent properties in all four dimensions, as illustrated in Fig. 1c, d, and Supplementary Fig. 1e (unless otherwise specified, the liquid content of AVD is 40%).

Nonetheless, a challenge of fabrication preexists in the application of gel dielectrics as the matrix of the emitting layer. The ZnS particles are prone to settle in the precursor liquid of the gel easily because of the density difference between the particles and the liquid. The rapid sedimentation behavior further induces dense packing at the bottom of the cured gel dielectrics. Therefore, the emission layer with homogeneously distributed ZnS particles is hard to obtain. Inspired by the dispersion of particles in polymer solutions, we increase the viscosity of the precursor liquid against the sedimentation process. A small amount of PVP (polyvinyl pyrrolidone) is thereby added to the precursor liquid. As shown in Fig. 1e, the viscosity of the precursor liquid is significantly increased from 7.19 mPa·s to 92.57 mPa·s. The ZnS particles are well suspended in the liquid with 3% PVP. Accordingly, the ZnS particles are homogeneously distributed in the cured gel dielectric, which is confirmed by the image of the confocal laser scanning microscope (CLSM) in Fig. 1a. We also evaluate the influence of PVP on the dielectric gel. The addition of PVP does not affect the key parameters of the gel, including dielectric constant, transmittance and stretchability, as depicted in Supplementary Fig. 2a–c. The dielectric gels with PVP additive could thus be mixed with ZnS to prepare the emitting layer, called APEL (unless otherwise specified, the ZnS content is 70 wt%), which were characterized in Supplementary Fig. 2d, e.

Stretchable devices with ultra-low-field emission

The APEL is fabricated in stretchable ACEL devices with stretchable electrodes, called APELSD. The devices are very bright because of the high- k dielectric gel, as shown in Fig. 1f and Fig. 2a–e. The APELSDs are categorized into APELSD-200, APELSD-500 and APELSD-800 according to the thickness of the emitting layer, APEL, 200, 500, and 800 μm . A typical three-layer sandwich structure is used to evaluate the performance, in which the carbon nanotube (CNT) coated polydimethylsiloxane (PDMS) is employed as a transparent and stretchable electrodes (Supplementary Fig. 2f). Under the same operating electric field (E), the electric fields (E_f) that across the ZnS particles are significantly enhanced, owing to the high dielectric constant of the dielectric, as shown in the simulation of Fig. 2a. On the contrary, the E_f is weakened by the regular elastomers with low dielectric constant. Therefore, the luminance of APELSD is very high. Notably, APELSD-800 reaches a very high luminance of $1823.5 \pm 167.0 \text{ cd m}^{-2}$ at the E of $2.5 \text{ V } \mu\text{m}^{-1}$ (Voltage = 2000 V) with 1 kHz, as shown in Supplementary Table 1. The luminance is increased with the thickness of the emitting layer and has a positive correlation with the applied electric fields, as illustrated in Fig. 2b and Supplementary Fig. 3a, b. Notably, the APELSD demonstrated the highest luminance compared to all previously reported intrinsically stretchable ACEL devices at similar operating conditions, as compared in Fig. 1f and Supplementary Table 1.

The turn-on threshold voltage of ACEL devices depends deeply on the dielectric constant and the thickness of the emitting layer. To date, the lowest turn-on threshold E of previous works is $0.34 \text{ V } \mu\text{m}^{-1}$ (Voltage = 23 V) with 50 Hz, which is achieved by a plasticized fluoroelastomer¹¹. Herein, we prepare an APELSD with a similar thickness of 70 μm (APELSD-70) to demonstrate the ultra-low turn-on voltage enabled by the high- k gel. The turn-on threshold of APELSD-70 is as low as $0.19 \text{ V } \mu\text{m}^{-1}$ (Voltage = 13 V) with 50 Hz, according to the curve of luminance *versus* V in Fig. 2c and Supplementary Fig. 3c. Meanwhile, a silicone-based ACEL is turned on by the $E = 1.05 \text{ V } \mu\text{m}^{-1}$ with 1 kHz, as shown in Supplementary Fig. 3d. The APELSD-70 reaches $81.3 \pm 0.7 \text{ cd m}^{-2}$ at a higher E of $2.5 \text{ V } \mu\text{m}^{-1}$ (175 V) while the silicone based device exhibits a much lower luminance of 3.5 cd m^{-2} . Such an applied frequency of 50 Hz is consistent with the utility frequency of power grid frequency (50 Hz or 60 Hz), allowing simpler power transformers in applications¹¹. Moreover, the turn-on electric field could be further reduced by the thicker emitting layer. The APELSD-800 can be lightened by an electric field as low as $0.11 \text{ V } \mu\text{m}^{-1}$ (Voltage = 88 V) with 50 Hz, as shown in Fig. 2c.

The content of ZnS in the emitting layer is also critical to the luminance because ZnS particles are the emitting centers for ACEL devices. Numerous works have reported that the dielectric constant of elastomers can be remarkably promoted by filler-doping methods³³. However, the limited space for loading ZnS caused by the fillers results in low efficacy for improving the luminance. In this work, the dielectric gel is free of additional fillers, and the ratio of ZnS thus reaches a high level. APELSD with three mass ratios of ZnS, 30, 50, and 70%, are investigated in Fig. 2d and Supplementary Fig. 3e–g. The brightness gradually increased with the rise of ZnS content. The simulation in Supplementary Fig. 3h reveals that the E_f is boosted at higher contents. Therefore, the higher density of emitting centers as well as the enhanced E_f simultaneously contribute to the higher luminance. The CIE coordinates are also recorded and showcase a typical Blue emission of ACEL devices at high applied frequencies (Supplementary Fig. 3i). Besides, as displayed in Supplementary Fig. 4, the dielectric constant of the gel can be adjusted from 16.6 to 56.8 (1 kHz) via the changing of liquid content from 10% to 40%. As a result, the E_f is promoted by the increment of the dielectric constant. Accordingly, the luminance of corresponding ACEL devices is stepwise enhanced, as presented in Fig. 2e, and Supplementary Fig. 4.

Next, we evaluate the mechanical properties of the APELSD. The APELSD displays a working stretchability of 80%, as shown in Fig. 2f–h.

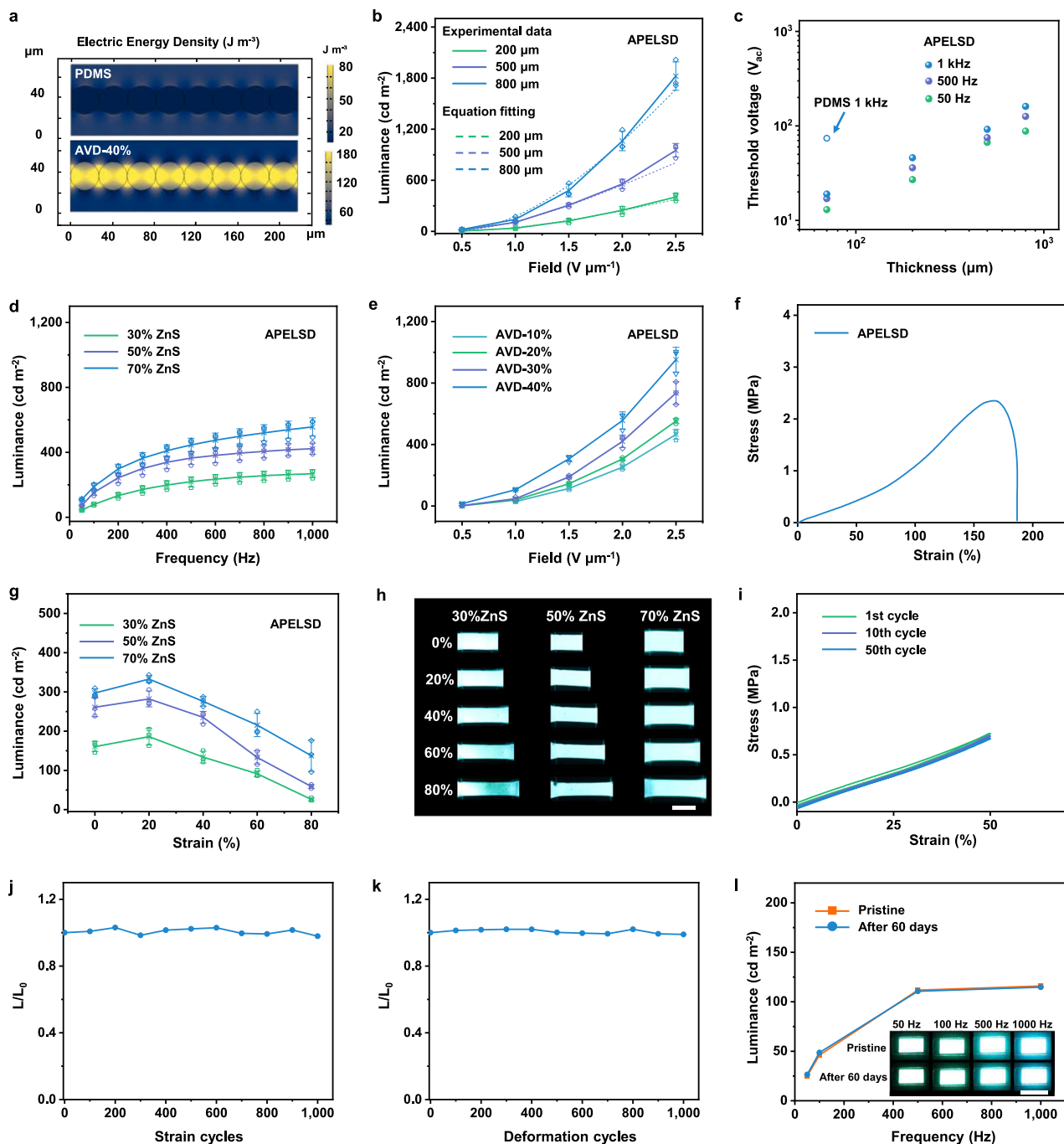


Fig. 2 | The luminance and mechanical performances of APELSD. **a** The COMSOL simulation of the ZnS doped dielectric gel and PDMS. **b** The luminance of APELSD with the different thicknesses under various driving electric fields. The dashed lines are the fitting lines according to equation $L = L_0 \exp(-(b/E)^{0.5})$, in which L represents the luminance, E denotes the electric field, and L_0 and b are constants. Data points represent mean \pm SD ($n = 3$). **c** The turn-on voltage of APELSD. The turn-on threshold luminance is 0.1 cd m^{-2} . **d** The luminance of APELSD-500 with the different ratios of ZnS particles at various frequencies. Data points represent mean \pm SD ($n = 3$). **e** The luminance of APELSD with different solvent contents

under various driving electric fields at 1 kHz. Data points represent mean \pm SD ($n = 3$). **f** The stress-strain curve of the APELSD. **g** The luminance (data points represent mean \pm SD, $n = 3$) and **(h)** digital photo (scale bar, 2 cm) of APELSD with the different ratios of ZnS particles as a function of strain. Data points represent mean \pm SD ($n = 3$). **i** Cyclic stress-strain curves of APELSD for 50 cycles at 50% strain. **j** Relative luminance (L/L_0) for strain cycling to 50% strain. **k** L/L_0 for different deformation cycles, including twisting, bending and stretching. **l** Luminance stability over 60 days. The digital photos at the initial states and after 60 days are also listed.

Although previous works reported very bright devices with high stretchability, the maximum stretchability of those devices relied on unrecoverable plastic deformation, and the elastic deformations was very small^{1,11}. However, the elastic stretchability of devices is more important for practical applications because the devices are expected to recover initial states after stretching. In terms of the APELSD, the

high- k gel is a crosslinked gel with intrinsically high stretchability. Therefore, the APELSD could be totally recovered after it is stretched to the maximum working elongation of 80%. Moreover, we evaluate the stability of APELSD via the cyclical stretching test, as shown in Fig. 2i–k. No liquid leakage is observed in these stability tests, ensuring stable luminance performance. The APELSD does not display an

obvious difference in luminance even after 1000 cycles at 50% strain or 1000 deformations, as demonstrated in Supplementary Movie 1 and Movie 2. We notice that such cyclical performance precedes that of many similar intrinsically stretchable optoelectronics with high brightness^{1,11,16}. The stability over time of APELSD is also assessed in a test period of 60 days, as presented in Fig. 2l. The luminance is maintained during the whole test period. In a 12 h continuous experiment, the luminance remains unchanged, also demonstrating good stability, (Supplementary Fig. 5a). Furthermore, the device functions normally in environments ranging from -10°C to 50°C . After VHB encapsulation, it maintains stable operation even under high humidity or immersion in saline solution (Supplementary Fig. 5b, c).

Full-color devices through fluorescent electrodes

Full color is highly desired because it can provide human beings with rich information^{5,41}. However, the color of ZnS-based ACEL devices is not satisfactory due to the limitation of ZnS particles⁵. Herein, we prepare electrodes with photoluminescence to achieve full-color ACEL devices through a simple yet very efficient method⁴². The preparation of electrodes is the doping substrate of electrodes with fluorescent particles. As shown in Fig. 3a, the photoluminescent electrodes are employed as the front electrode, while the back electrode is still selected as the transparent electrode. The Blue (B) light from the emitting layer is absorbed and blocked by the photoluminescent electrode and further converted into desired photoluminescence, as illustrated Fig. 3b, c, and Supplementary Fig. 6. Accordingly, the front layer can achieve multiple colors through different fluorescent particles, Yellow (Y, 0.32,0.60), Green (G, 0.24,0.56), and Red (R, 0.57,0.38). Combined with the original Blue color (B, 0.18, 0.35), the full-color devices are thus achieved, as shown in Fig. 3d. In the meantime, the colors on the backsides come from the mixed light of the photoluminescence from the front electrode and the blue light from the emitting layer (Supplementary Fig. 6). The device could thus afford Janus colors for display. Moreover, this method exploits the indispensable electrode and does not need to change the structure of ACEL devices, demonstrating a general strategy for colorful ACEL devices.

The luminance can be further improved by the photoluminescent electrodes. The backsides are brighter because of the mixed light, as shown in Fig. 3e–h and Supplementary Fig. 7a–d. The highest brightness reaches to $1944.7 \pm 99.4 \text{ cd m}^{-2}$ at a low $E = 2.5 \text{ V } \mu\text{m}^{-1}$ with 1 kHz for APELSD-800 with yellow electrode, as shown in Fig. 3e. Besides, the thinner APEL is more efficient to enhance the luminance of backside because the higher transmittance of APEL allows more photoluminescence to cross, as illustrated in Fig. 3e, f and Supplementary Fig. 7e. The luminance of the backsides increased to 1.52 folds, 1.33 folds, 1.15 folds, and 1.07 folds respectively, as the APEL are gained from $70 \mu\text{m}$ to $800 \mu\text{m}$. The luminance of the backside could also be enhanced by the Red and Green electrodes because of the mixed light, as demonstrated in Fig. 3g, h, and Supplementary Fig. 7c, d. In terms of the fronts, the luminance of the fronts is reduced due to the blocking effect of the electrodes. Nevertheless, the luminance of the front (APELSD-500) is still maintained at a high level compared with other reported works, as shown in Supplementary Table 1^{11,30}. The stretchability performance of colorful APELSD is recorded in Fig. 3i–k and Supplementary Fig. 7f. As expected, the devices still work well within 80% strain because the structure is unchanged. The cyclical stability is assessed in Supplementary Fig. 7g, h. Neither the colors nor the luminance shows significant changes under 1000 cyclical strains at 50%.

Highly stretchable APELSD with gel electrodes

Moreover, the stretchability of APELSD could be enhanced by replacing the CNT-coated PDMS with a more stretchable gel electrode, as shown in Fig. 4a. To cooperate with the light-emitting layer of gel, additional elastomer layers are inserted to separate the emitting layer

with the gel electrode, forming a five-layer device (called APELSD-F). The inserted layer is a transparent acrylate-based elastomer (PBA) with a maximum elongation of $682 \pm 53\%$, while the gel electrode is a conductive deep eutectic solvent (DES) gel with $976 \pm 76\%$ elongation (Supplementary Fig. 8a–d). PBA is also employed to load ZnS particles at the same content as the emitting layer to maximize its utilization. The APELSD-F with 70% ZnS could be elastically stretched up to 200%, owing to the good stretchability of all layers as well as good interfacial stickiness, as shown in Fig. 4b and Supplementary Fig. 8e. The APELSD-F exhibits slightly lower brightness compared with the three-layer APELSD, achieving a maximum luminance of $1311.1 \pm 114.1 \text{ cd m}^{-2}$ at $2.5 \text{ V } \mu\text{m}^{-1}$ (Fig. 4c and Supplementary Fig. 8f–i). This reduction in brightness is attributed to the lower dielectric constant of the inserted layer, which is 5.7 at 1 kHz (Supplementary Fig. 9a, b). Nevertheless, the brightness of APELSD-F remains highly outstanding when compared with previously reported stretchable ACEL devices, as shown in Supplementary Table 1. Besides, the electrode thickness ($300 - 800 \mu\text{m}$) does not affect the luminous performance of the devices (Supplementary Fig. 9c).

The elongation could be further enhanced by reducing the content of ZnS, as presented in Fig. 4b, d–f and Supplementary Fig. 10. The APELSD-F with 30% ZnS reaches a large deformation over 600% and emits stably in such process, Fig. 4b and Supplementary Movie 3. As for the cyclic performance, the APELSD-F also behaves well in a cyclic test at 200% strain on account of the intrinsic stretchability of all layers. More importantly, the luminance is also very steady in the cyclic test. As displayed in Fig. 4f and Supplementary Movie 4, the APELSD-F maintains its brightness compared to its original value even after stretching for 1000 cycles to 200% strain. In general, the APELSD avoids the plasticized materials usually used in the high-brightness stretchable optoelectronics, demonstrating outstanding stretchability in practical application.

Dynamical display through wireless communications

Wearable display holds promising potential for interactive information that is the foundation of versatile integrated flexible electronics systems. As presented in Fig. 5a–c, a display device with an 8×16 pixel array is developed, enabling real-time dynamic information display via Bluetooth communication. The pixels are formed at the crossings of front and back electrode strips. Moreover, the multiple colors are also integrated into the array by the photoluminescent electrodes in the front. Those photoluminescent electrodes enable the array with Janus colors in two faces. The Red, Blue, Green, and Yellow emerge in the front, while the Blue appears in the back accordingly. The array is controlled by a microcontroller with a dynamic scanning method. As the wireless communication is established between the array and the smartphone, the real-time dynamic display can be realized. As shown in Fig. 5d and Supplementary Movie 5, the color array exhibits content received from smartphones, including characters like “20”, “25”, “BE”, “ST”, various patterns, and other custom information. In bending states, the device also functions well to display the characters “1234”, indicating good flexibility, as illustrated in Fig. 5a. Generally, the colorful array demonstrates a practical wearable display device for effective information interaction and establishes a solid foundation for other integrated flexible electronics systems.

In summary, we present a dielectric gel that enables a stretchable ACEL device with very high brightness. For the four key dimensions of the emission layers of ACEL devices, the dielectric gel exhibits excellent overall performance: a high dielectric constant of $56.8 @ 1 \text{ kHz}$, a high transmittance of $93\% @ 550 \text{ nm}$, a good stretchability of $961 \pm 61\%$, and a large space for particle loading. Such a result delegates the ACEL devices with an ultra-low turn-on voltage of 13 V and a large elongation up to 600%. The maximum luminance could achieve $1944.7 \pm 99.4 \text{ cd m}^{-2}$ at a low applied electric field of $2.5 \text{ V } \mu\text{m}^{-1}$. Moreover, fluorescent electrodes are introduced, and corresponding Red,

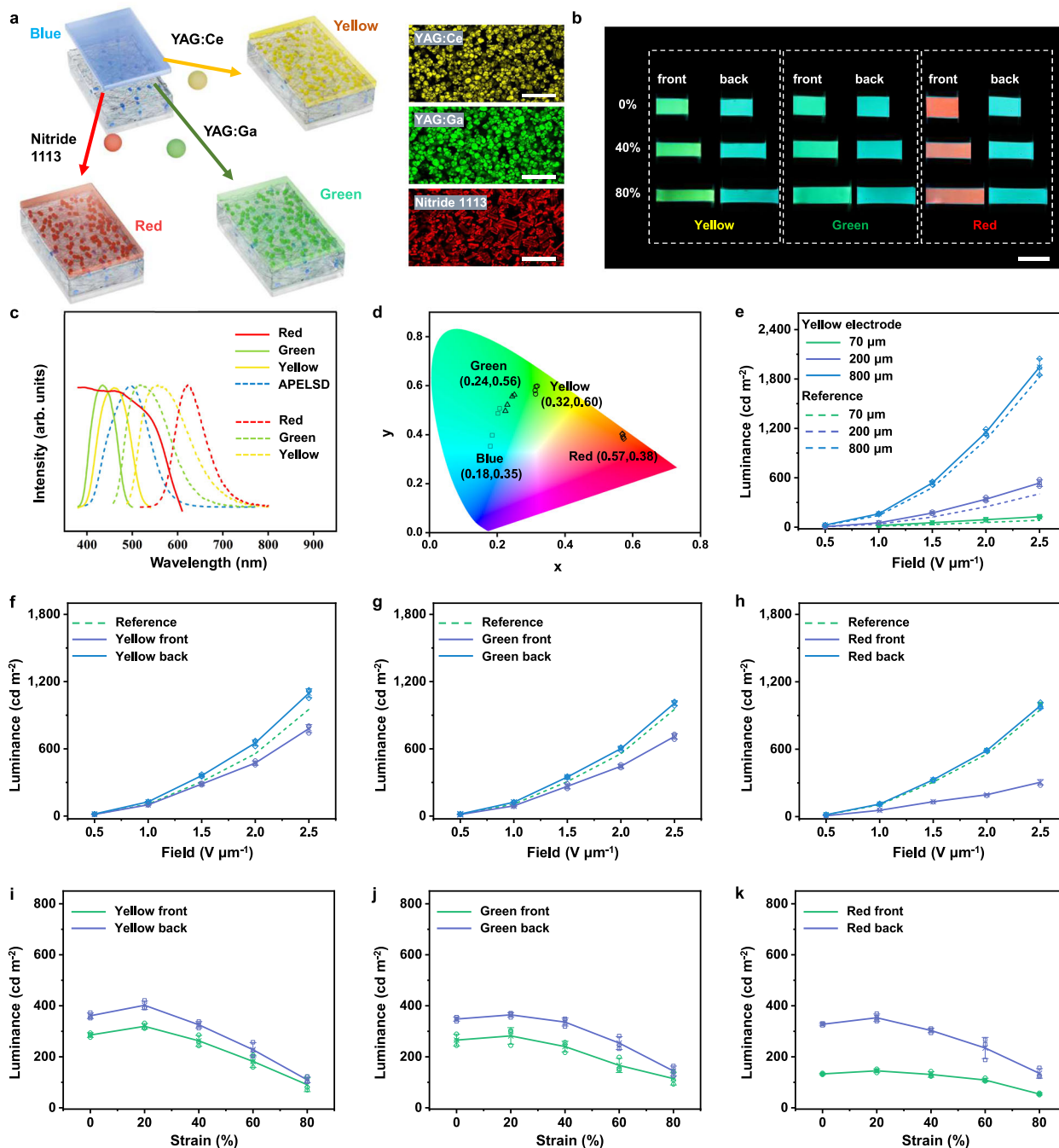


Fig. 3 | The colors and luminescence of APELSD based on photoluminescent electrodes. **a** Structure of stretchable APELSD with various photoluminescent electrodes. Images are the laser confocal characterization of the photoluminescent electrode. Scale bar, 100 μm . **b** The digital photos of different photoluminescent electrode devices under stretching. Scale bar, 3 cm. **c** Excitation spectra of the Red, Green, and Yellow electrodes. The emission spectrum of the APELSD without photoluminescent electrodes is the dashed line. The emission spectra of the Red, Green and Yellow electrodes are also in dashed line. **d** The CIE coordinates of APELSD with different photoluminescent electrodes under various driving

frequencies, 50 Hz \sim 1 kHz. **e** The backside luminescence of APELSD with a Yellow electrode with the different thicknesses of APEL. The dashed lines are corresponding APELSD without photoluminescent electrodes for references. The luminance of APELSD-500 with (f) Yellow, (g) Green and (h) Red electrodes under various driving electric fields. The dashed lines are APELSD-500 without photoluminescent electrodes for references. The luminance of APELSD-500 with the (i) Yellow, (j) Green and (k) Red electrodes as a function of strain. Data points in Fig. 3e–k represent mean \pm SD ($n = 3$).

Yellow, Green could be achieved without additional or complicated structure designs. A colorful stretchable display is further fabricated, which can dynamically display designed signals in real time through Bluetooth communication. This work demonstrated the potential of the dielectric gel for ACEL devices and could significantly promote the advancement of stretchable optoelectronics, particularly for stretchable displays for human-machine interactions.

Methods

Materials and characterization

Choline chloride (ChCl), ethylene glycol (EG), acrylic acid (AA), 4-vinyl-1,3-dioxolan-2-one (VEC), poly(ethylene glycol) diacrylate (PEGDA, Mw: 1000), 2-hydroxy-2-methylpropiophenone (photo-initiator 1173), polyvinylpyrrolidone (PVP, K88-96), and single-walled carbon nanotubes (SWCNTs, OD: < 2 nm, Length: 5–30 μm) were the

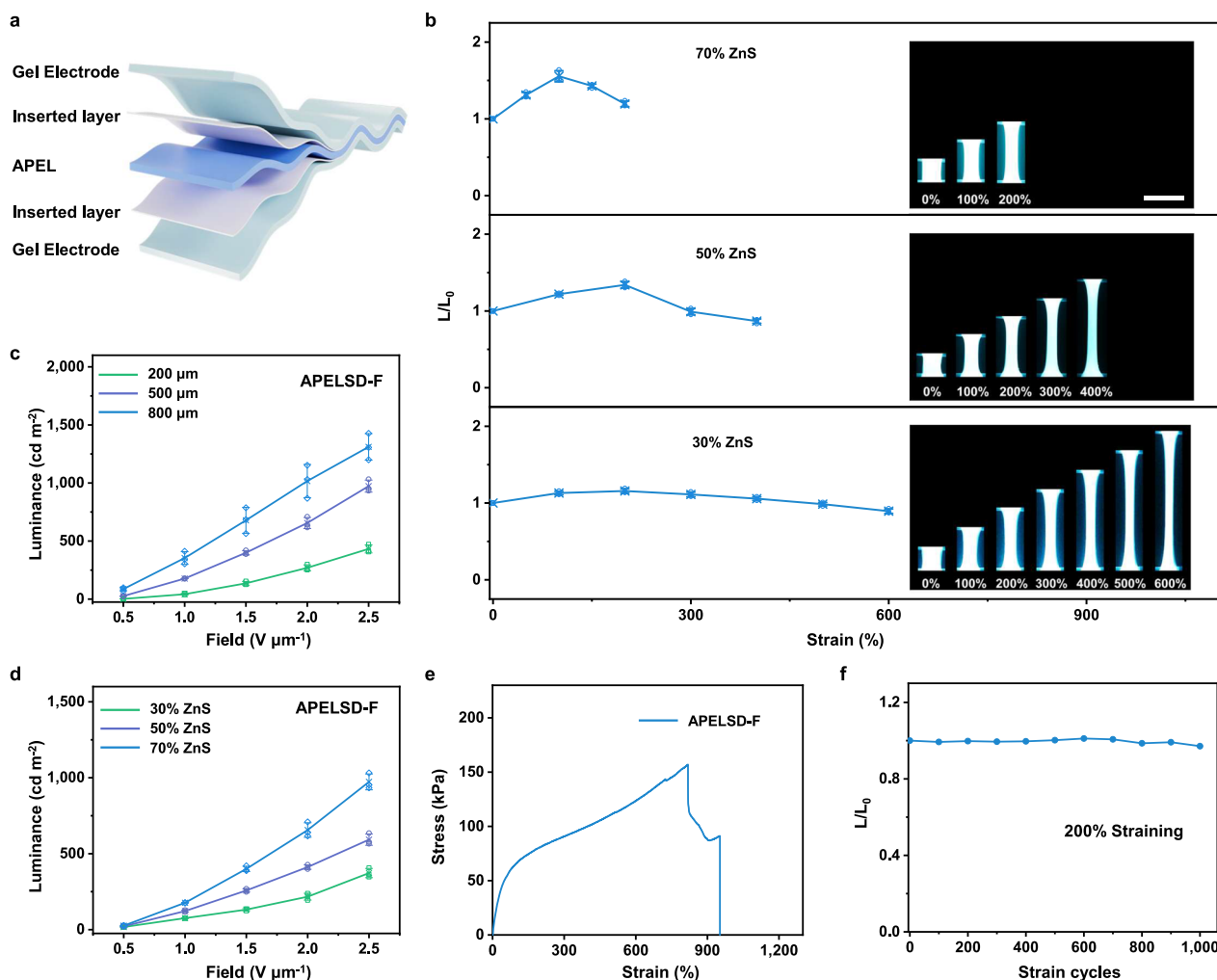


Fig. 4 | Gel electrodes enabled devices with a higher elongation based on a five-layer structure. **a** Structure of ultra-stretchable APELSD-F. **b** The L/L_0 of APELSD-F with different ratios of ZnS particles as a function of strain. The inserted figures illustrate the stretching ability of APELSD-F. Scale bar, 3 cm. **c** The luminance of APELSD-F with multiple thicknesses under various driving electric fields. **d** The

luminance of APELSD-F with different ratios of ZnS particles under various driving electric fields. Data points in Fig. 4b–d represent mean \pm SD ($n = 3$). **e** The stress-strain curve and **(f)** L/L_0 for cyclic strain of 200% of the APELSD-F. The content of ZnS is 30% and the thickness of APEL is 500 μm .

chemicals of Shanghai Macklin Biochemical Technology Co., Ltd. 4-acryloylmorpholine (ACMO), butyl acrylate (BA), octadecyltrichlorosilane (OTS), and 1-hydroxycyclohexyl phenyl ketone (photoinitiator 184) were the reagents of Shanghai Aladdin Bio-Chem Technology Co., Ltd. Propylene carbonate (PC) and ethylene carbonate (EC) were the reagents of Alfa Aesar Chemical Co., Ltd. PDMS (Sylgard 184) was the elastomer product of Dow Corning. Electroluminescent phosphor (ZnS:Cu) were acquired from Shanghai KPT Co., Ltd. Photoluminescent microparticles (YAG:Ce, yellow, YG-45M; YAG:Ga, green, GG-520B; Nitride 1113, red, HR-629H) were made by Grirum Advanced Materials Co., Ltd. CN9021 was the macro-crosslinker from Sartomer Co., Ltd. Isopropanol (IPA) was used to dilute the SWCNT, adjusting its concentration to 0.3 mg mL^{-1} . A 90 min sonication was needed for SWCNT dispersion. All chemicals were utilized directly as received, with no additional purification performed.

We used the Confocal White Laser Scanning microscopy (Leica STELLARIS 5) to observe the emitting layer and the fluorescent electrode. The dielectric properties were assessed with the aid of a broadband dielectric/impedance spectrometer (Concept 50, Novocontrol Technologies GmbH&Co.KG). The FTIR data were measured by a machine of Nicolet iS50-Nicolet RaptIR, Thermo Scientific. The

mechanical properties were recorded by a universal testing machine (HZ-1007C, Dongguan Lixian Instrument Technology Co., Ltd.) at a constant stroke speed of 50 mm min^{-1} . The sample sizes of the tensile test were: APEL (thickness: 0.5 mm, length: 15 mm, width: 8 mm), gels (thickness: 1 mm, length: 15 mm, width: 8 mm). The transparency test was conducted on a UV-Vis/NIR spectrophotometer (UH-5700, Hitachi) equipped with a 60-mm integrating sphere. The gel specimens were measured to be 1 mm thick. The emitting layer and CNT/PDMS electrode samples were found to have a thickness of 0.5 mm. The vacuum laminator is the machine of JKD-LH18F, Shenzhen Jingke Machinery & Electronic Equipment Co., Ltd.

The ACEL device was driven by an alternating current signal (square wave), which was generated by a function waveform generator (33509B, Keysight) and amplified by a high-voltage amplifier (EEL1102.05, EEL). Luminescent properties, including luminance values, emission spectra, and CIE coordinates, were tested by a luminance meter (SRC-200M, Everfine). The excitation fluorescence spectra data were recorded through a photoluminescence spectrometer (FLS1000, Edinburgh Instruments). Tensile and cycle tests on the stretchable ACEL device were conducted using a linear translation stage. The stretchable ACEL display was operated by a drive system consisting of a microcontroller (Arduino, STM32) and a Bluetooth

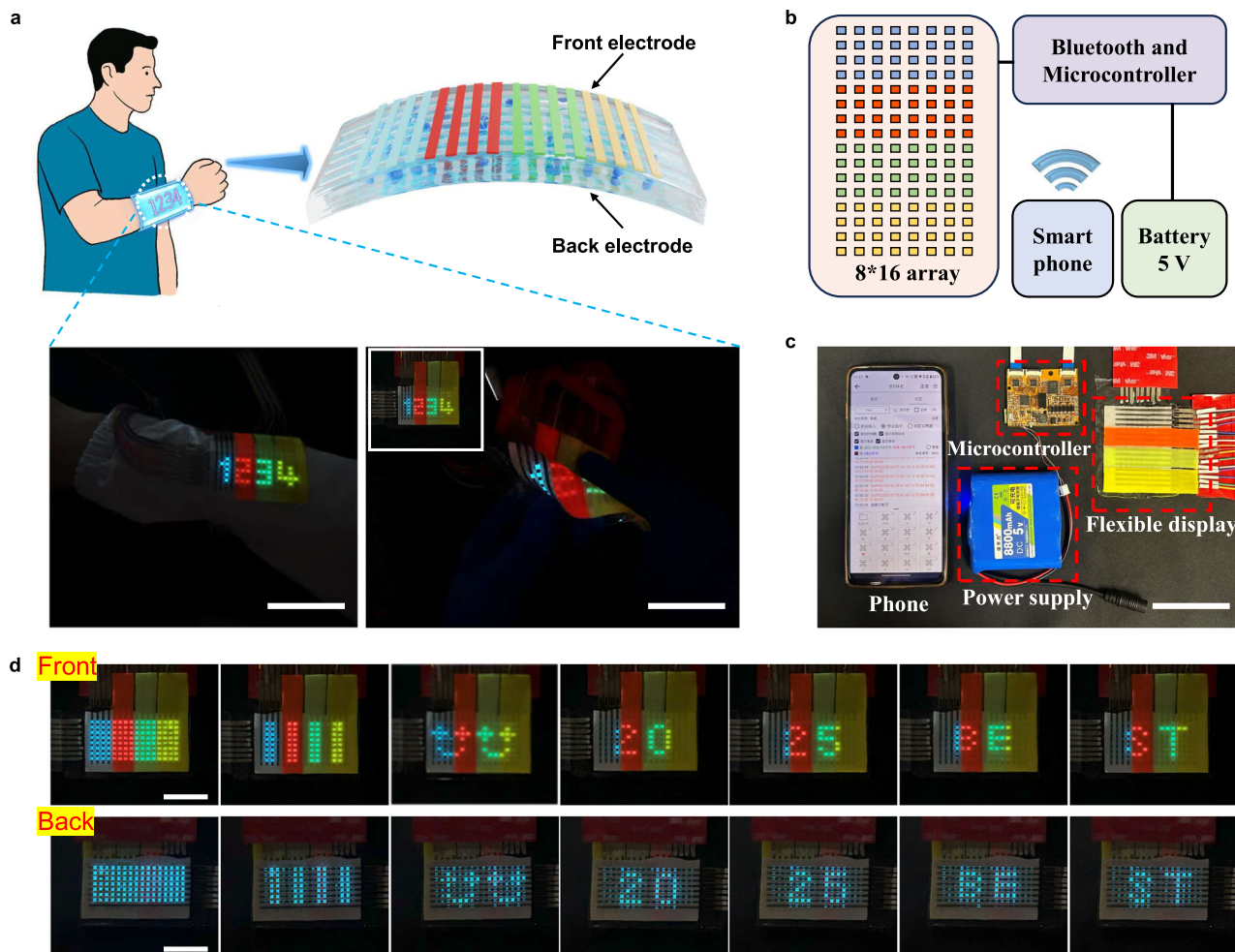


Fig. 5 | Colorful display with 128 pixels for real-time dynamic display. **a** The full-color device of 8*16 pixels displays the information through wireless communications. The inserted digital photo shows the “1234” number received from the smartphone. Scale bar = 6 cm for the left photo. Scale bar = 5 cm for the right photo.

b The system-level block diagram and **(c)** the Digital photo of the full-color wireless display show the module connected to the microcontroller, which is powered by a 5 V battery. Scale bar, 6 cm. **d** Dynamic information is displayed on the front and back of the full-color display. Scale bar, 3 cm.

module. The microcontroller can generate a voltage of 190 V_{p-p} with 2 kHz. The system was powered by a 5 V lithium battery (Jiangmen Baofengli New Energy Technology Co., Ltd.). All data involving mean values are derived from distinct samples.

Preparation of dielectric gel (AVD) and emitting layer APEL

The monomers for gel preparation were the mixture of ACOM and VEC (molar ratio was 1:1), while the swelling solvent for gel is the mixed liquid of EC and PC with a 4:1 volume ratio. The precursor solution was composed of monomer and swelling solvent at designed weight ratios (0% - 40% swelled solvent). The crosslinker and photoinitiator 184 were used at 0.1%, and 1.5% molar ratios of the total amount of the monomers, respectively. The precursor liquid of gel was thus obtained. For APEL, PVP was further added at a content of 3 wt% of the precursor liquid of gel. After that, the precursor liquid of emitting layer was obtained by the introduction of ZnS: Cu particles at designed ratios with 30 min sonication. The precursor liquid was poured into a transparent glass mold with silicone spacers and release films. After 15 minutes of UV irradiation (420 nm, 50 W), a dielectric gel or emitting layer was obtained. The thickness was controlled by adjusting the silicone spacer.

Preparation of electrodes

Transparent CNT/PDMS electrodes were fabricated by the deposition of SWCNT on a transparent PDMS film (thickness of 0.5 mm) via a spray

coating method. The area density of SWCNT was approximately 90 μg cm⁻². The fluorescent electrodes were produced by replacing the transparent PDMS film with a fluorescent PDMS film. The fluorescent PDMS film was fabricated by the mixture of precursor solution of PDMS and photoluminescent phosphor microparticles at corresponding mass fractions. The preparation method for the ultra-stretchable DES gel electrodes was a typical gel preparation: First, ChCl and EG were mixed at a 1:2 molar ratio and stirred at 80 °C until a transparent and uniform liquid was formed, resulting in a deep eutectic solvent (DES). Next, the pre-gel solution was obtained by mixing the monomer AA, crosslinker PEGDA, photoinitiator 1173, and DES. The DES content was fixed at 50 wt%, and the molar ratios of crosslinker and photoinitiator to monomer were fixed at 0.07% and 0.5%, respectively. The solution was then poured into a transparent glass mold with a silicone spacer and release films. UV irradiation (365 nm, 300 W, 5 min) was performed to prepare the conductive DES-gel electrode.

Fabrication of ACEL devices

The three-layer ACEL device consists of an APEL sandwiched between two CNT/PDMS electrodes. For the three-layer fluorescent ACEL device, one of the transparent CNT/PDMS electrodes is replaced with a fluorescent electrode. For the ultra-stretchable ACEL device with five layers, both the front and back sides of the APEL were coated with an

isolation layer of approximately 100 μm . The isolation layer was a ZnS doped elastomer, which was prepared by UV curing (10 min, 420 nm, 50 W) of CN9021 and BA in a 1:1 mass ratio. The content of ZnS in the isolation layer was the same as that of APEL. The emitting layer with the isolation layers was then sandwiched between two 1 mm thick DES-gel electrodes to form the ultra-stretchable ACEL device.

Preparation of stretchable ACEL array displays

For the array display, parallelly and equally spaced CNT/PDMS electrodes were fabricated by an OTS-modified glass through a mask spray coating method (8 or 16). A layer of PDMS was first cured on the glass surface to form an 8-array PDMS@SWCNT electrode. In the same procedure, pure PDMS was replaced with a mixture of PDMS and fluorescent powder to form a fluorescent electrode with a 16-array. Next, a prepared APEL with 110 μm thickness was sandwiched between the two electrode arrays in a perpendicular way. Finally, the assembled device was laminated at 60 kPa for 5 min to ensure a strong bond between the layers, resulting in an 8*16 array display.

Density functional theory calculations

The structures of monomer and dimer were obtained via first-principles calculations, which were carried out in Vienna ab initio simulation package (VASP) within the framework of density-functional theory^{43,44}. The cutoff energy of basic plane wave functions was set to 600 eV. The exchange-correlation functions were described by the generalized gradient approximation within Perdew-Burke-Ernzerhof (PBE) formalism⁴⁵. The convergence for the forces was set to smaller than 0.01 eV-Å⁻¹.

Reporting summary

Further information on research design is available in the Nature Portfolio Reporting Summary linked to this article.

Data availability

All data generated in this study are available in this article and in the Supplementary Information or from the corresponding authors upon request. The data have been deposited in the Source data file. Source data are provided in this paper.

References

- Zhang, Z. T. et al. High-brightness all-polymer stretchable LED with charge-trapping dilution. *Nature* **603**, 624–630 (2022).
- Zhang, Z., Wang, Y., Jia, S. & Fan, C. Body-conformable light-emitting materials and devices. *Nat. Photon.* **18**, 114–126 (2023).
- Lee, J. H., Cho, K. & Kim, J. K. Age of flexible electronics: emerging trends in soft multifunctional sensors. *Adv. Mater.* **36**, e2310505 (2024).
- Zhou, H. Y., Kim, H. W., Jeong, W. J. & Lee, T. W. Toward intrinsically stretchable OLEDs with high efficiency. *Adv. Mater.* **37**, e2420008 (2025).
- Chun, F. et al. Multicolour stretchable perovskite electroluminescent devices for user-interactive displays. *Nat. Photon.* **18**, 856–863 (2024).
- Zhang, P. et al. Integrated 3D printing of flexible electroluminescent devices and soft robots. *Nat. Commun.* **13**, 4775 (2022).
- Zhang, Z. & Bao, Z. High luminescent polymers for stretchable displays. *Natl. Sci. Rev.* **10**, nwac093 (2023).
- Jiang, W., Lee, S., Zan, G., Zhao, K. & Park, C. Alternating Current Electroluminescence for Human-Interactive Sensing Displays. *Adv. Mater.* **36**, e2304053 (2023).
- Fu, X. M. et al. Self-healing actuatable electroluminescent fibres. *Nat. Commun.* **15**, 10498 (2024).
- Wang, X. et al. Coplanar pattern and temperature transient control in intelligent wearable multi-color alternating current electroluminescence devices. *Adv. Funct. Mater.* **35**, 2420613 (2025).
- Tan, Y. J. et al. A transparent, self-healing and high-dielectric for low-field-emission stretchable optoelectronics. *Nat. Mater.* **19**, 182–188 (2020).
- Li, X. C. et al. Intrinsically stretchable electroluminescent elastomers with self-confinement effect for highly efficient non-blended stretchable OLEDs. *Angew. Chem. Int. Ed. Engl.* **62**, e202213749 (2023).
- Yoo, J., Li, S., Kim, D. H., Yang, J. & Choi, M. K. Materials and design strategies for stretchable electroluminescent devices. *Nanoscale Horiz.* **7**, 801–821 (2022).
- Song, H. et al. Water stable and matrix addressable OLED fiber textiles for wearable displays with large emission area. *Npj Flex. Electron.* **6**, 66 (2022).
- Kim, D. C. et al. Intrinsically stretchable quantum dot light-emitting diodes. *Nat. Electron.* **7**, 365–374 (2024).
- Jeong, M. W. et al. Intrinsically stretchable three primary light-emitting films enabled by elastomer blend for polymer light-emitting diodes. *Sci. Adv.* **9**, eadh1504 (2023).
- Zhang, X. & Wang, F. Recent advances in flexible alternating current electroluminescent devices. *Appl. Mater.* **9**, 030701 (2021).
- Wang, Z., Shi, X. & Peng, H. S. Alternating current electroluminescent fibers for textile displays. *Natl. Sci. Rev.* **10**, nwac113 (2023).
- Fang, T. et al. Hybrid liquid metal/ionic nanocomposite transparent electrodes for highly stretchable electroluminescent matrix displays. *Adv. Funct. Mater.* **35**, 2417982 (2025).
- Luo, Z. Q. et al. Fully Printable and reconfigurable -type electroluminescent devices for visualized encryption. *Adv. Mater.* **36**, e2313909 (2024).
- Zhang, K. L. et al. Design and fabrication of wearable electronic textiles using twisted fiber-based threads. *Nat. Protoc.* **19**, 1557–1589 (2024).
- Shi, X. et al. Large-area display textiles integrated with functional systems. *Nature* **591**, 240–245 (2021).
- Cho, S. S., Chang, T., Yu, T. H., Gong, S. L. & Lee, C. H. Machine embroidery of light-emitting textiles with multicolor electroluminescent threads. *Sci. Adv.* **10**, eadk4295 (2024).
- Oh, S. J. et al. Stretchable multicolored electroluminescent sound display for wearable and interactive textiles. *Adv. Funct. Mater.* **24**, 2420432 (2025).
- Stauffer, F. & Tybrandt, K. Bright stretchable alternating current electroluminescent displays based on high permittivity composites. *Adv. Mater.* **28**, 7200–7203 (2016).
- Feng, Q. K. et al. Recent progress and future prospects on all-organic polymer dielectrics for energy storage capacitors. *Chem. Rev.* **122**, 3820–3878 (2022).
- Dang, Z. M., Yuan, J. K., Yao, S. H. & Liao, R. J. Flexible nanodielectric materials with high permittivity for power energy storage. *Adv. Mater.* **25**, 6334–6365 (2013).
- Zhou, Y. L. et al. Stretchable high-permittivity nanocomposites for epidermal alternating-current electroluminescent displays. *ACS Mater. Lett.* **1**, 511–518 (2019).
- Zhang, C., Bao, Q., Zhu, H. & Zhang, Q. Highly transparent and long-term stable dielectric elastomer composites enabled by poly(ionic liquid) inclusion. *Adv. Funct. Mater.* **34**, 2401901 (2024).
- Liu, Y., Sun, L., Feng, W., Jin, Z. & Wang, C. A stable, self-healable, and stretchable dielectric polymer for electroluminescent device working underwater. *Adv. Funct. Mater.* **34**, 2402453 (2024).
- Wood, V. et al. Inkjet-printed quantum dot-polymer composites for full-color AC-driven displays. *Adv. Mater.* **21**, 2151–2155 (2009).
- Huang, J., Zhang, X., Liu, R., Ding, Y. & Guo, D. Polyvinyl chloride-based dielectric elastomer with high permittivity and low viscoelasticity for actuation and sensing. *Nat. Commun.* **14**, 1483 (2023).
- Yang, M. et al. Polymer nanocomposite dielectrics for capacitive energy storage. *Nat. Nanotechnol.* **19**, 588–603 (2024).

34. Pan, C. et al. A liquid-metal-elastomer nanocomposite for stretchable dielectric materials. *Adv. Mater.* **31**, e1900663 (2019).
35. Hu, L. et al. Hydrogel-based flexible electronics. *Adv. Mater.* **35**, e2205326 (2023).
36. Go, Y. et al. Optically transparent and mechanically robust ionic hydrogel electrodes for bright electroluminescent devices achieving high stretchability over 1400%. *Adv. Funct. Mater.* **33**, 2215193 (2023).
37. Dinh Xuan, H. et al. Super stretchable and durable electroluminescent devices based on double network ionogels. *Adv. Mater.* **33**, e2008849 (2021).
38. Shi, L. et al. Dielectric gels with ultra-high dielectric constant, low elastic modulus, and excellent transparency. *Npg Asia Mater.* **10**, 821–826 (2018).
39. Seward, R. P. & Vieira, E. C. The dielectric constants of ethylene carbonate and of solutions of ethylene carbonate in water, methanol, benzene and propylene carbonate. *J. Phys. Chem.* **62**, 127–128 (1958).
40. Hall, D. S., Self, J. & Dahn, J. R. Dielectric constants for quantum chemistry and Li-ion batteries: solvent blends of ethylene carbonate and ethyl methyl carbonate. *J. Phys. Chem. C.* **119**, 22322–22330 (2015).
41. Zhu, Y. et al. Bright bifacial white-light illumination by highly deformable electroluminescent devices based on transparent ionic-hydrogel electrodes and quantum-dot color conversion. *Small* **20**, 2400704 (2024).
42. Liu, Z. et al. Full-color, highly bright and stretchable electroluminescent device with Janus colors based on photoluminescent electrode for wireless dynamical display. *Compos. Part B Eng.* **286**, 111787 (2024).
43. Kohn, W. & Sham, L. J. Self-consistent equations including exchange and correlation effects. *Phys. Rev.* **140**, A1133–A1138 (1965).
44. Kresse, G. & Furthmüller, J. Efficient iterative schemes for ab initio total-energy calculations using a plane-wave basis set. *Phys. Rev. B* **54**, 11169–11186 (1996).
45. Perdew, J. P., Burke, K. & Ernzerhof, M. Generalized gradient approximation made simple. *Phys. Rev. Lett.* **77**, 3865–3868 (1996).

Acknowledgements

The authors acknowledge the funding support from the National Natural Science Foundation of China (project numbers: 52203153, T.J.) for the work reported here.

Author contributions

T.J. conceived and supervised this work. T.J. and Z.L. (Zupeng Liu) co-designed the experiments. Z.L. (Zupeng Liu) performed the major

experiments to obtain the data. Z.L. (Zhao Liu) carried out the DFT calculations. X.L. measured some samples, including tensile testing and light emission spectral measurements. Y.Y. conducted the COMSOL simulation, some luminance tests and schematic diagrams. T.J. wrote the draft. Z.L. (Zupeng Liu), Y.Y., and Z.L. (Zhao Liu) all contributed to the paper writing for the final version of the manuscript.

Competing interests

The authors declare no competing interests.

Additional information

Supplementary information The online version contains supplementary material available at <https://doi.org/10.1038/s41467-025-66206-9>.

Correspondence and requests for materials should be addressed to Yujue Yang or Titao Jing.

Peer review information *Nature Communications* thanks Cheolmin Park and the other anonymous reviewer(s) for their contribution to the peer review of this work. A peer review file is available.

Reprints and permissions information is available at <http://www.nature.com/reprints>

Publisher's note Springer Nature remains neutral with regard to jurisdictional claims in published maps and institutional affiliations.

Open Access This article is licensed under a Creative Commons Attribution-NonCommercial-NoDerivatives 4.0 International License, which permits any non-commercial use, sharing, distribution and reproduction in any medium or format, as long as you give appropriate credit to the original author(s) and the source, provide a link to the Creative Commons licence, and indicate if you modified the licensed material. You do not have permission under this licence to share adapted material derived from this article or parts of it. The images or other third party material in this article are included in the article's Creative Commons licence, unless indicated otherwise in a credit line to the material. If material is not included in the article's Creative Commons licence and your intended use is not permitted by statutory regulation or exceeds the permitted use, you will need to obtain permission directly from the copyright holder. To view a copy of this licence, visit <http://creativecommons.org/licenses/by-nc-nd/4.0/>.

© The Author(s) 2025